Zintl Clusters

Deutsche Ausgabe: DOI: 10.1002/ange.201508246
Internationale Ausgabe: DOI: 10.1002/anie.201508246

Zintl Clusters as Wet-Chemical Precursors for Germanium Nanomorphologies with Tunable Composition

Manuel M. Bentlohner, Markus Waibel, Patrick Zeller, Kuhu Sarkar, Peter Müller-Buschbaum, Dina Fattakhova-Rohlfing, and Thomas F. Fässler**

Abstract: *$[Ge_9]^{4-}$ Zintl clusters are used as soluble germanium source for a bottom–up fabrication of Ge nanomorphologies such as inverse opal structures with tunable composition. The method is based on the assembly and oxidation of $[Ge_9]^{4-}$ clusters in a template mold using $SiCl_4$, $GeCl_4$, and PCl_3 leading to Si and P-containing Ge phases as shown by X-ray diffraction, Raman spectroscopy, and energy-dispersive X-ray analysis. $[Ge_9]^{4-}$ clusters are retained using ethylenediamine (en) as a transfer medium to a mold after removal of the solvent if water is thoroughly excluded, but are oxidized to amorphous Ge in presence of water traces. ^1H NMR spectroscopy reveals the oxidative deprotonation of en by $[Ge_9]^{4-}$. Subsequent annealing leads to crystalline Ge. As an example for wet-chemical synthesis of complex Ge nanomorphologies, we describe the fabrication of undoped and P-doped inverse opal-structured Ge films with a rather low oxygen contents. The morphology of the films with regular volume porosity is characterized by SEM, TEM, and grazing incidence small-angle X-ray scattering.*

Group 14 element semiconductors such as Si and Ge are important materials in optoelectronic industry with a mature fabrication technology. Commercially available morphologies are dominated by bulk, thin film, and nanocrystalline forms, but the needs of emerging applications boost interest in other types of nanoarchitectures. Particularly, nanoparticles, nanowires and porous forms of Group 14 semiconductors attract significant attention because of a broad range of potential applications such as electrochemical energy storage, sensing, photovoltaics, microelectronics, and photonics.[1]

Synthetic approaches to manufacture Group 14 nanoparticles[2] and nanowires[3] are well-established, but the routes to the periodic porous materials are much more scarce. Porous Si or Ge layers are mainly obtained by chemical or electrochemical etching of corresponding dense materials providing a good control over the composition and crystallinity, but only a limited control over the porous structure and the surface chemistry.[1f,4] In this respect, bottom–up approaches based on the solidification of molecular precursors are more beneficial for fabricating periodic porous materials with an unprecedented control over the shape, size, and spatial arrangement of the pores. Numerous bottom–up approaches have been developed for metal oxides resulting in a large library of periodic porous morphologies.[5] However, an extension of these methods to the fabrication of non-oxide materials faces serious challenges and is mainly limited by the availability of suitable precursors capable of solidification to porous scaffolds in a controllable way. So far only a limited number of techniques to fabricate non-oxide porous semiconductors has been reported, such as chemical vapor deposition (CVD) involving silanes/germanes,[6] electrochemical reduction of Group 14 halides[7] and reduction of Ge^{IV} oxide with hydrogen or alkali metals.[8]

Several years ago germanium Zintl clusters have been introduced as precursors for nanostructured non-oxide semiconductors.[9,13a,g] Zintl clusters are polyanionic cages, which emerge in intermetallic compounds between alkaline or alkaline-earth metals and p-block (semi)metals. The solubility of Zintl phases in selected solvents, a rich library of compositions, and the possibility of coupling those units[10] make Zintl clusters attractive, versatile precursors for fabrication of non-oxide nanostructures with tunable composition and electronic properties.[11] Soluble Zintl clusters were used for electrodeposition of dense Ge layers[12] as well as for fabrication of mesoporous powders[13] and films[14] of Group 14–16 elements using surfactant-templating approaches. Despite of the expected potential of Zintl clusters as nanostructure precursors, today the number of reported applications is still rather low. The key problem is that the chemistry of the involved reactions is largely unclear, thereby restricting the generalization of these methods to diverse template morphologies and fabrication scales.

Here we present the application of $[Ge_9]^{4-}$ Zintl clusters as Ge source for the fabrication of Ge nanomorphologies with tunable composition by their controlled solidification to a solid phase, which is compatible with the controlled formation of complex morphologies (Figure 1). Specifically, our approach involves the transfer and homogenous distribution of the Zintl phase K_4Ge_9 in a template mold and the purposefully initiated oxidation of the $[Ge_9]^{4-}$ clusters. In order to gain control over this process we have additionally

[*] M. M. Bentlohner, Dr. M. Waibel, Prof. Dr. T. F. Fässler
Department Chemie, Technische Universität München
Lichtenbergstraße 4, 85747 Garching (Germany)
E-mail: thomas.faessler@lrz.tu-muenchen.de
P. Zeller, Priv.-Doz. Dr. D. Fattakhova-Rohlfing
University of Munich (LMU) and Center for NanoScience (CeNS)
Butenandtstrasse 5–13 (Haus E), 81377 München (Germany)
E-mail: dina.fattakhova@cup.uni-muenchen.de
Dr. K. Sarkar, Prof. Dr. P. Müller-Buschbaum
Physik-Department, Lehrstuhl für Funktionelle Materialien
Technische Universität München
James-Franck-Straße 1, 85748 Garching (Germany)

Supporting information for this article including all experimental details as well as extensive descriptions of the experimental data is available on the WWW under http://dx.doi.org/10.1002/anie.201508246. Video material is available under https://vimeo.com/76125397.

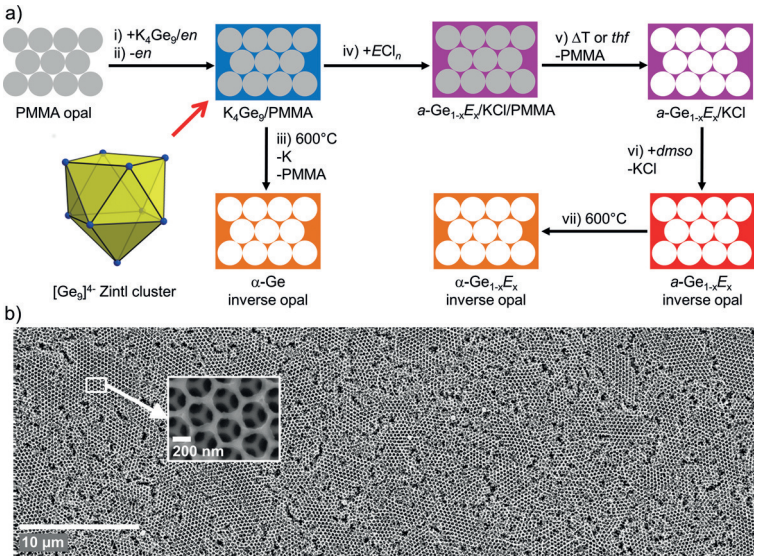

Figure 1. a) Fabrication of Ge inverse opals (INOP) by controlled oxidation of $[Ge_9]^{4-}$ Zintl clusters, (i) Infiltration of a polymethylmethacrylate (PMMA) opal (grey spheres) with K_4Ge_9/en, ii) evaporation of en, iii) annealing of the K_4Ge_9/PMMA composite at 600 °C and formation of crystalline α-Ge INOP and K vapor, iv) impregnation of K_4Ge_9/PMMA composite with ECl_n (E = Si, Ge, P) and formation of amorphous a-$Ge_{1-x}E_x$ (purple), v) removal of PMMA by flash-annealing or dissolution in tetrahydrofuran (thf), vi) removal of KCl with dimethylsulfoxid (dmso), vii) annealing of a-$Ge_{1-x}E_x$-INOP and formation of α-$Ge_{1-x}E_x$ INOP (orange). b) Scanning electron micrographs of a-$Ge_{1-x}Ge_x$ INOP and magnified section of the film as inlay.

conducted a series of ex situ experiments to investigate the transfer of $[Ge_9]^{4-}$ Zintl clusters into the templates and the cluster oxidation chemistry.

As transfer medium en, a common solvent for $[Ge_9]^{4-}$, was used.[11] Even though the previous publications hypothesize the possible role of en as an oxidant for K_4Ge_9,[10–11,13d–f] the experimental evidences for such a process have never been provided. We found that removal of en from a K_4Ge_9/en solution leads directly to amorphous Ge (a-Ge) through the oxidation of dissolved $[Ge_9]^{4-}$ Zintl clusters by en (Figure 2b). However, this reaction only takes place in the presence of traces of water,[15] which triggers the oxidation of the Zintl anions. For the first time deprotonation of en was confirmed using ^{1}H NMR spectroscopy (see Figure S4 in the Supporting Information), evidencing an oxidizing potential of en towards $[Ge_9]^{4-}$ clusters. Such a process has been previously proposed for the formation of Ge_9 dimers, oligomers, and polymers such as $[Ge_9{=}Ge_9{=}Ge_9{=}Ge_9]^{8-}$.[10,16] In contrast to that, removal of en from completely water-free K_4Ge/en-solutions (see the Supporting Information for the details of the en distillation) leads to the conservation of the polyhedral clusters as demonstrated by Raman spectroscopy (Figure 2a).

Thus, under meticulous exclusion of water, en is a suitable medium for the non-destructive transfer of K_4Ge_9 into the template molds, offering possibilities of their further transformations to solid Ge phase. One of such transformations is the oxidation of $[Ge_9]^{4-}$ Zintl clusters through thermal annealing (Figure 2c). Therefore, K_4Ge_9 recovered from a water-free en solution by the removal of solvent was annealed for 5 minutes at 500 °C in vacuo and subsequently for 1 h at 600 °C in argon resulting in crystalline Ge (α-Ge).[17] This process is accompanied by the release of elemental potassium visible as a metal mirror deposited on the colder parts of the recipient (Figure S2). Furthermore, the presence of intact Zintl clusters enables their cross-linking with ECl_n (E = Si, Ge, n = 4; E = P, n = 3; Figure 2d). Because of the high Lewis acidity of the positively polarized E atom in ECl_n, such halides react readily with the highly Lewis basic $[Ge_9]^{4-}$ clusters. This route is particularly attractive for nanostructure assembly as it proceeds at ambient conditions and, more importantly, enables tuning of composition and controllable doping by introducing different elements.[13a–c,f,14] Because of a vigorous reaction of ECl_n with en the latter should be thoroughly removed prior to the contact with ECl_n. In the ex situ experiments the cross-linking between the K_4Ge_9 and ECl_n (E = Si, Ge, n = 4; E = P, n = 3) was investigated in toluene, which is inert towards both compounds. The relevant XRD patterns of the obtained reaction products point to the formation of potassium chloride and an amorphous phase (see the powder diffractograms in Figures S5–S7, the Raman spectra in Figure S5, and the results of EDX in Table S1). The presence of potassium chloride is indicative for

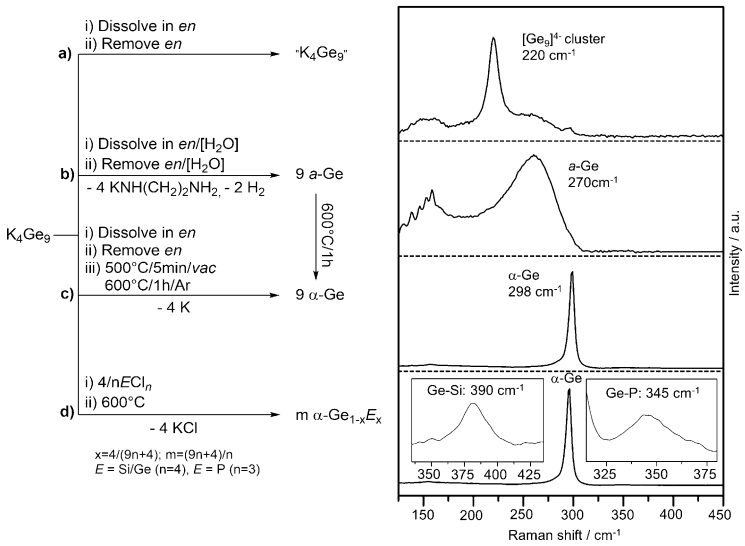

Figure 2. Ex situ investigations on the oxidation of $[Ge_9]^{4-}$ Zintl clusters (left: reaction schemes, right: Raman spectra, reference data see refs. [18–21]). Evaporating solutions of K_4Ge_9 in a) water-free en retains $[Ge_9]^{4-}$ clusters, but the same procedure in b) en containing water traces forms a-Ge which transforms to α-Ge at 600 °C; c) as a) and subsequent annealing forms α-Ge and K vapor, d) reaction of K_4Ge_9 with ECl_n (E = Si, Ge; n = 4; E = P, n = 3). KCl is removed with dmso, α-$Ge_{1-x}E_x$ forms at 600 °C. For details see Figures S2–S7.

the successful cross-linking reaction according to the reaction scheme in Figure 2d. The amorphous phase crystallizes by annealing at 600 °C, as follows from the XRD patterns as well as the Raman spectra. The use of heteroatomic linkers, different from Ge, enables incorporation of silicon or phosphorous into the Ge structure. When $SiCl_4$ is used as linker, the XRD reflections of the crystalline product are shifted to higher angles,[22] and in Raman spectra an additional signal at 390 cm^{-1} is detected corresponding to the Ge–Si vibrational mode.[20] For the product cross-linked with PCl_3, the Ge–P mode at 345 cm^{-1}[21] is visible in the Raman spectra. K/Cl/Ge/*E* (*E* = Si, P) atomic ratios obtained by energy-dispersive X-ray analysis (EDX) of the amorphous and crystallized products are in a good agreement with the expected stoichiometry of the cross-linking reactions.

Nanostructured materials are inherently fragile and thus the minimization of mechanical stress during fabrication is required. Generally, the application of gaseous reagents comes along with less mechanical stress compared to the application of solutions. Hence, representative for other volatile cross-linkers, we investigated the gas-phase reaction of $GeCl_4$ vapors with the bulk K_4Ge_9. Similar to the reaction in toluene described above, potassium chloride and Ge was formed, pointing to the applicability of the gas-phase oxidation method for the film fabrication.

As an example of the suitability of Zintl clusters for wet-chemical synthesis of complex Ge nanomorphologies using the oxidation reactions discussed above, we describe the fabrication of undoped and phosphorous-doped inverse opal-structured Ge films (Figure 1 and Figure S8). In contrast to the recently reported electrodeposition method for inverse opal structures,[7] the wet-chemical impregnation protocol followed by a controlled solidification described in this work is not limited to the conducting substrates, leads to nanostructured compounds with tunable composition and with lower oxygen content, and is universally applicable to any kind of morphologies with different shapes and dimensions. Ge films with an inverse opal structure are prepared by colloidal crystal templating using periodic arrays of polymethylmethacrylate (PMMA) beads as the templates for porosity. Dried composite films obtained after infiltration of PMMA opal template with a solution of K_4Ge_9 in en contain $[Ge_9]^{4-}$ clusters as follows from the Raman spectra. Zintl clusters periodically distributed in template voids can be transformed to a solid Ge phase with similar nanomorphology using either thermal treatment or cross-linking reaction routes described above. In a thermal procedure, the dried films are annealed for 5 minutes at 500 °C in vacuo and for one hour at 600 °C in Ar, resulting in the pyrolysis of PMMA,[23] release of elemental potassium and formation of mechanically stable crystalline macroporous Ge films (α-Ge-INOP). Alternatively, $[Ge_9]^{4-}$ Zintl clusters distributed in template voids can be cross-linked to form the solid phase. Treatment of the dried $[Ge_9]^{4-}$/PMMA composites in $GeCl_4$ vapor results in the formation of 3D-Ge network distributed in the PMMA bead matrix. PMMA can be removed by a gentle dissolution in thf, although the resulting macroporous films are rather fragile. Mechanical stability of the Ge networks is significantly improved after flash-annealing (5 minutes at 500 °C) in vacuo. Raman spectra of the resulting films show a broad signal at 270 cm^{-1} typical for the amorphous Ge (*a*-$Ge_{1-x}Ge_x$ INOP).[19b] KCl formed as a side product of this reaction is washed out by extracting the films with dmso. EDX analysis of such films proves that the framework consists entirely of Ge and that KCl is efficiently removed.

Scanning electron microscopy (SEM) images of the films obtained by both methods show the same inverse opal structure. In addition, perfect ordering of the inverse opal films is confirmed by grazing incidence small-angle X-ray scattering (GISAXS) experiments that gives insights into the volume morphology of the porous frameworks (detailed description of GISAXS data see Figure S11).[24] GISAXS scattering patterns show two types of periodicity with a d-spacing of 203 nm (called further pore A) and 151 nm (called pore B), which gives an evidence of a long-range periodicity in the bulk of the macroporous film. The porous structure parameters obtained by SEM and GISAXS are in a good agreement with the TEM results (Figure 3), which show uniformly sized periodic pores with the diameter of 150 nm and 200–250 nm corresponding to B pores and A pores, respectively.

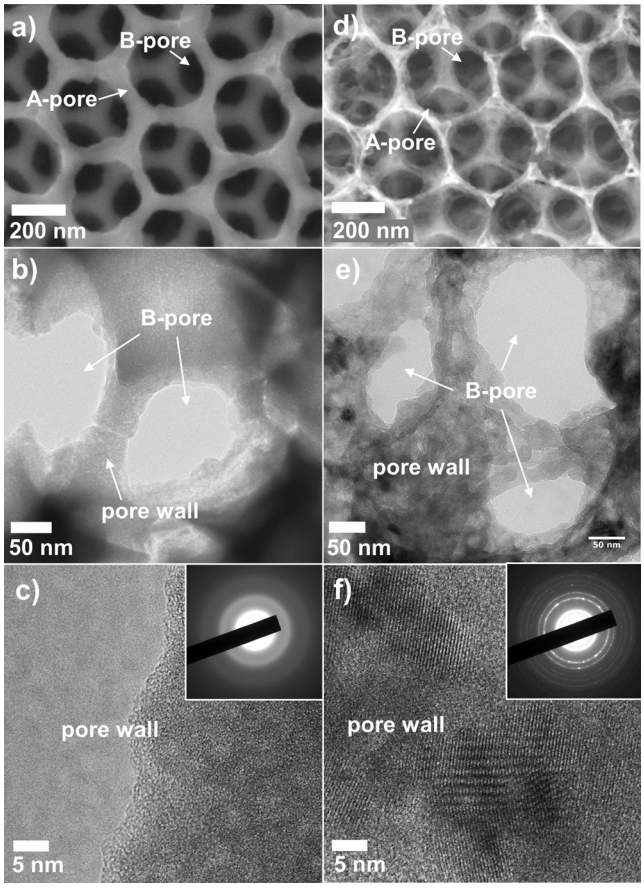

Figure 3. SEM and TEM images of a–c) *a*-$Ge_{1-x}Ge_x$-INOP and d–f) α-$Ge_{1-x}Ge_x$-INOP; a) and d) SEM (pore types A and B are depicted); b) and e) low-magnification TEM; c) and f) high-resolution TEM; insets c) and f) selected-area electron diffraction pattern.

The macroporous Ge scaffolds obtained by the low-temperature cross-linking of Zintl clusters are amorphous up to 500 °C, as follows from the Raman spectroscopy measurements, high-resolution TEM images (HR-TEM, Figure 3c) and selected-area electron diffraction (SAED) measurements in TEM. Aiming for the same inverse opal-structured Ge but with the enhanced crystallinity, the amorphous films were annealed for one hour at 600 °C in argon atmosphere (α-$Ge_{1-x}Ge_x$-INOP). SEM images of this film (Figure 3d) show that the inverse opal structure withstands annealing at 600 °C. The pore wall thickness decreases after annealing because of the densification of the Ge scaffold. TEM images (Figure 3e–f) as well as the SAED pattern (Figure 3f inset) of the film annealed at 600 °C reveal that the pore walls consist of crystalline Ge nanoparticles with the size of around 10–20 nm embedded in an amorphous matrix. Consequently, in the Raman spectrum a sharp peak at 298 cm^{-1} appears, corresponding to the optical phonon mode of crystalline Ge. Powder XRD patterns of the films scraped off the substrate display reflections of α-Ge (Figure S9). The size of the crystalline domains calculated from the broadening of individual lines using the Scherrer equation corresponds to 10–15 nm, in good agreement with the TEM analysis.

X-ray photoelectron spectra (XPS) of the annealed films (Figure 4) display signals of Ge^0 (binding energy Ge^0 3d orbital: 29.7 eV) and much lower signals of GeO and GeO_2 (binding energies: +1.8 eV and +3.4 eV with respect to Ge^0 3d, respectively).[25] Contributions from GeO and GeO_2 to both the $2p_{3/2}$ and 3d signals are significantly reduced by sputtering the films with Ar^+ ions, indicating that Ge oxides are present only at the surface of the porous framework (for details on the interpretation of the XPS spectra see Figures S12/S13). Therefore, the macroporous Ge scaffolds obtained from the Zintl clusters consist of Ge^0 and only little GeO and GeO_2, in contrast to electrodeposited Ge morphologies.[7d]

For the application of Ge in electronic devices doping is required.[26] To demonstrate the possibility of incorporating dopants into the porous Ge scaffold by our cross-linking method, we have treated $[Ge_9]^{4-}$/PMMA composite with PCl_3 vapor and annealed the film (600 °C/1 h) to remove PMMA and enhance the crystallinity (α-$Ge_{1-x}P_x$-INOP). SEM images of the washed films display the same regular porosity as the films obtained by cross-linking with $GeCl_4$, but the EDX analysis reveals the presence of phosphorous (Figure S8). Similar to the ex situ experiments with PCl_3 described above, the Raman spectra of the films show an additional signal at 345 cm^{-1} corresponding to the Ge–P vibration (Figure S10),[21] which indicates that phosphorous was incorporated into the porous Ge scaffold by PCl_3 cross-linking. The possibility to solidify clusters both by thermal annealing and cross-linking gives the possibility to control the amount of introduced dopants.

The presented results highlight the large potential of $[Ge_9]^{4-}$ Zintl clusters as Ge source for the versatile and controlled chemical fabrication of Ge morphologies. The detailed ex situ investigations on the transfer and controlled oxidation of $[Ge_9]^{4-}$ Zintl clusters and step-by-step monitoring of the transfer reactions provide the basis for a rational and general fabrication method for complex Ge nanomorphologies and the possibility of targeted composition tuning, as it is shown for the formation of highly ordered inverse opal structures. Currently we are running tests to apply the PMMA and K_4Ge_9/en solution by spin- and spray-coating on different types of substrates in order to achieve large-area inverse opal-structured films. The as-obtained inverse opal-structured films are tested for applications in hybrid solar cells and as thin film anodes. Moreover, our investigations outline that our method can be transferred to other types of Zintl compounds such as soluble $[Ge_{9-x}Si_x]^{4-}$ Zintl anions providing a versatile fabrication technique for nanostructured silicon films.

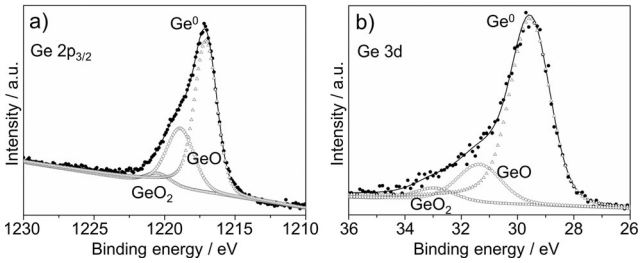

Figure 4. XPS spectra of *a*-$Ge_{1-x}Ge_x$-INOP after 20 min of sputtering with Ar^+ ions. a) Ge $2p_{3/2}$ and b) Ge 3d signal. Data points (circles), fitted curve (solid line). Contributions of Ge (triangles), GeO (rhombs), GeO_2 (squares).

Experimental Section

Fabrication of Ge INOP films: A PMMA opal (for the fabrication see the Supporting Information) was infiltrated with a solution of K_4Ge_9 in en grade A (concentration 50 mg mL^{-1}) by drop casting. The dried K_4Ge_9/PMMA composite was either annealed: 5 min/500 °C/in vacuo, 1 h/600 °C/Ar or treated with $GeCl_4$ or PCl_3 vapor at room temperature for one week or longer in a glass vessel, respectively. PMMA was removed either by dissolution in thf or flash-annealing (5 minutes at 500 °C in vacuo). KCl was removed by extracting the films for 1 h with dmso. The films were crystallized at 600 °C/1 h.

Acknowledgements

The authors thank for funding this work the research network "Solar Technologies go Hybrid" (State of Bavaria) via TUM.solar and LMU Center Materials for Renewable Energies, the NIM cluster (DFG) and the Center for Nano-Science (CeNS). We thank M.Sc. Michael Giebel, M.Sc. Sebastian Geier, and M.Sc. Kristina Peters for help with the preparation of the Ge INOP films and PMMA. The authors are grateful to Dr. Sigrid Bernstorff from the Elettra-Sincrotrone Trieste S.C.p.A for help during the setting-up of the GISAXS experiment, to Dr. Steffen Schmidt and Dr. Benjamin Mandlmeier, University of Munich (LMU), for electron microscopy, as well as to Dipl.-Phys. Benedikt Stoib and Prof. Dr. Martin Brandt, Walter Schottky Institute, for fruitful discussions. We also thank M.Sc. Marius Loch and Prof. Dr. Paolo Lugli, Technical University of Munich, for first tests on applying spin- and spray-coating methods.

Keywords: composition tuning · germanium · inverse opals · nanostructuring · zintl clusters

How to cite: *Angew. Chem. Int. Ed.* **2016**, *55*, 2441 – 2445
Angew. Chem. **2016**, *128*, 2487 – 2491

[1] a) M.-H. Park, K. Kim, J. Kim, J. Cho, *Adv. Mater.* **2010**, *22*, 415 – 418; b) D. D. Vaughn II, R. E. Schaak, *Chem. Soc. Rev.* **2013**, *42*, 2861 – 2879; c) R. Pillarisetty, *Nature* **2011**, *479*, 324 – 328; d) K. Ramasamy, P. G. Kotula, A. F. Fidler, M. T. Brumbach, J. M. Pietryga, S. A. Ivanov, *Chem. Mater.* **2015**, *27*, 4640 – 4649; e) M. G. Kanatzidis, *Adv. Mater.* **2007**, *19*, 1165 – 1181; f) A. Stein, *Nature* **2006**, *441*, 1055 – 1056.

[2] a) X. D. Pi, U. Kortshagen, *Nanotechnology* **2009**, *20*, 295602; b) A. Fojtik, M. Giersig, A. Henglein, *Ber. Bunsen-Ges. Phys. Chem.* **1993**, *97*, 1493 – 1496; c) A. Dowd, R. G. Elliman, B. Luther-Davies, *Appl. Phys. Lett.* **2001**, *79*, 2327 – 2329; d) J. A. Kelly, E. J. Henderson, J. G. C. Veinot, *Chem. Commun.* **2010**, *46*, 8704 – 8718.

[3] M. Amato, M. Palummo, R. Rurali, S. Ossicini, *Chem. Rev.* **2014**, *114*, 1371 – 1412.

[4] H. C. Choi, J. M. Buriak, *Chem. Commun.* **2000**, 1669 – 1670.

[5] D. Fattakhova-Rohlfing, A. Zaleska, T. Bein, *Chem. Rev.* **2014**, *114*, 9487 – 9558.

[6] a) M. Seino, E. J. Henderson, D. P. Puzzo, N. Kadota, G. A. Ozin, *J. Mater. Chem.* **2011**, *21*, 15895 – 15898; b) H. Míguez, E. Chomski, F. Garcia-Santamaría, M. Ibisate, S. John, C. López, F. Meseguer, J. P. Mondia, G. A. Ozin, O. Toader, H. M. van Driel, *Adv. Mater.* **2001**, *13*, 1634 – 1637.

[7] a) R. Al-Salman, X. Meng, J. Zhao, Y. Li, U. Kynast, M. M. Lezhnina, F. Endres, *Pure Appl. Chem.* **2010**, *82*, 1673 – 1689; b) L. K. van Vugt, A. F. van Driel, R. W. Tjerkstra, L. Bechger, W. L. Vos, D. Vanmaekelbergh, J. J. Kelly, *Chem. Commun.* **2002**, 2054 – 2055; c) W. Xin, J. Zhao, D. Ge, Y. Ding, Y. Li, F. Endres, *Phys. Chem. Chem. Phys.* **2013**, *15*, 2421 – 2426; d) X. Meng, R. Al-Salman, J. Zhao, N. Borissenko, Y. Li, F. Endres, *Angew. Chem. Int. Ed.* **2009**, *48*, 2703 – 2707; *Angew. Chem.* **2009**, *121*, 2741 – 2745.

[8] a) H. Míguez, F. Meseguer, C. López, M. Holgado, G. Andreasen, A. Mifsud, V. Fornés, *Langmuir* **2000**, *16*, 4405 – 4408; b) J. Hwang, C. Jo, M. G. Kim, J. Chun, E. Lim, S. Kim, S. Jeong, Y. Kim, J. Lee, *ACS Nano* **2015**, *9*, 5299 – 5309; c) J. Liang, X. Li, Z. Hou, T. Zhang, Y. Zhu, X. Yan, Y. Qian, *Chem. Mater.* **2015**, *27*, 4156 – 4164; d) C. Zhang, Z. Lin, Z. Yang, D. Xiao, P. Hu, H. Xu, Y. Duan, S. Pang, L. Gu, G. Cui, *Chem. Mater.* **2015**, *27*, 2189 – 2194; e) H. Jia, R. Kloepsch, X. He, J. P. Badillo, P. Gao, O. Fromm, T. Placke, M. Winter, *Chem. Mater.* **2014**, *26*, 5683 – 5688.

[9] A. M. Guloy, R. Ramlau, Z. Tang, W. Schnelle, M. Baitinger, Y. Grin, *Nature* **2006**, *443*, 320 – 323.

[10] a) T. F. Fässler, *Angew. Chem. Int. Ed.* **2007**, *46*, 2572 – 2575; *Angew. Chem.* **2007**, *119*, 2624 – 2628; b) A. J. Karttunen, T. F. Fässler, M. Linnolahti, T. A. Pakkanen, *ChemPhysChem* **2010**, *11*, 1944 – 1950.

[11] S. Scharfe, F. Kraus, S. Stegmaier, A. Schier, T. F. Fässler, *Angew. Chem. Int. Ed.* **2011**, *50*, 3630 – 3670; *Angew. Chem.* **2011**, *123*, 3712 – 3754.

[12] N. Chandrasekharan, S. C. Sevov, *J. Electrochem. Soc.* **2010**, *157*, C140 – C145.

[13] a) G. S. Armatas, M. G. Kanatzidis, *Science* **2006**, *313*, 817 – 820; b) S. D. Korlann, A. E. Riley, B. L. Kirsch, B. S. Mun, S. H. Tolbert, *J. Am. Chem. Soc.* **2005**, *127*, 12516 – 12527; c) P. N. Trikalitis, K. K. Rangan, T. Bakas, M. G. Kanatzidis, *Nature* **2001**, *410*, 671 – 675; d) G. S. Armatas, M. G. Kanatzidis, *Adv. Mater.* **2008**, *20*, 546 – 550; e) G. S. Armatas, M. G. Kanatzidis, *Nano Lett.* **2010**, *10*, 3330 – 3336; f) G. S. Armatas, M. G. Kanatzidis, *J. Am. Chem. Soc.* **2008**, *130*, 11430 – 11436; g) S. Dong, A. E. Riley, A. J. Cadby, E. K. Richman, S. D. Korlann, S. H. Tolbert, *Nature* **2006**, *441*, 1126 – 1130.

[14] a) A. E. Riley, S. D. Korlann, E. K. Richman, S. H. Tolbert, *Angew. Chem. Int. Ed.* **2006**, *45*, 235 – 241; *Angew. Chem.* **2006**, *118*, 241 – 247; b) S. D. Korlann, A. E. Riley, B. S. Mun, S. H. Tolbert, *J. Phys. Chem. C* **2009**, *113*, 7697 – 7705.

[15] A detailed section on the purification and quality check of en is shown in the Supporting Information. We exploited the reaction of 7-amino-1-(trimethylsilyl)-5-aza-hepta-3-en – 1-yne[27] to 2,3-dihydro-5-methyl-1*H*-1,4-diazepine in en, which is triggered by water, to qualitatively check the water content of the solvent.

[16] a) C. Downie, Z. J. Tang, A. M. Guloy, *Angew. Chem. Int. Ed.* **2000**, *39*, 337 – 340; *Angew. Chem.* **2000**, *112*, 346 – 348; b) L. Yong, S. D. Hoffmann, T. F. Fässler, *Z. Anorg. Allg. Chem.* **2004**, *630*, 1977 – 1981.

[17] An identical annealing procedure as for en treated K_4Ge_9, was applied to neat crystalline K_4Ge_9. Thereby a mixture of K_8Ge_{44} and α-Ge was obtained.

[18] H. G. Von Schnering, M. Baitinger, U. Bolle, W. Carrillo-Cabrera, J. Curda, Y. Grin, F. Heinemann, J. Llanos, K. Peters, A. Schmeding, M. Somer, *Z. Anorg. Allg. Chem.* **1997**, *623*, 1037 – 1039.

[19] a) S. Schlecht, M. Yosef, M. Froba, *Z. Anorg. Allg. Chem.* **2004**, *630*, 864 – 868; b) J. Fortner, R. Q. Yu, J. S. Lannin, *J. Vac. Sci. Technol. A* **1990**, *8*, 3493 – 3495.

[20] H. H. Burke, I. P. Herman, *Phys. Rev. B* **1993**, *48*, 15016 – 15024.

[21] N. Fukata, K. Sato, M. Mitome, Y. Bando, T. Sekiguchi, M. Kirkham, J.-i. Hong, Z. L. Wang, R. L. Snyder, *ACS Nano* **2010**, *4*, 3807 – 3816.

[22] L. Vegard, *Z. Kristallogr.* **1928**, *67*, 239.

[23] S. M. Al-Salem, P. Lettieri, J. Baeyens, *Waste Manage.* **2009**, *29*, 2625 – 2643.

[24] a) P. Müller-Buschbaum, *Anal. Bioanal. Chem.* **2003**, *376*, 3 – 10; b) G. Renaud, R. Lazzari, F. Leroy, *Surf. Sci. Rep.* **2009**, *64*, 255 – 380.

[25] D. Schmeisser, R. D. Schnell, A. Bogen, F. J. Himpsel, D. Rieger, G. Landgren, J. F. Morar, *Surf. Sci.* **1986**, *172*, 455 – 465.

[26] C. Claeys, E. Simoen, *Germanium-Based Technologies: From Materials to Devices*, Elsevier Science, Amsterdam, **2011**.

[27] M. M. Bentlohner, W. Klein, Z. H. Fard, L.-A. Jantke, T. F. Fässler, *Angew. Chem. Int. Ed.* **2015**, *54*, 3748 – 3753; *Angew. Chem.* **2015**, *127*, 3819 – 3824.

Received: September 3, 2015
Revised: October 4, 2015
Published online: December 3, 2015

